International Journal of Thermophysics, Vol. 13, No. 4, 1992

A New Microsecond Pulse-Heating System to Investigate Thermophysical Properties of Solid and Liquid Metals

E. Kaschnitz,[1] G. Pottlacher,[1] and H. Jäger[1]

Received February 10, 1992

A new discharge system for resistive self-heating has been constructed for the measurement of accurate thermophysical properties. A constant-current pulse is used to heat metals over a time interval of 50 to 100 μs, reaching temperatures up to the boiling point. New techniques have been developed to obtain sound speeds in the pulse-heated sample, emissivities, and vapor pressure. A new pyrometer allows the extension of the measured temperature range down to the melting point of copper.

KEY WORDS: dynamic measurements; emissivity; high temperatures; liquid metals; nickel; pulse heating; sound velocity; tungsten.

1. INTRODUCTION

At the First Workshop on Subsecond Thermophysics in Gaithersburg, Maryland [1], a group of panelists discussed the key issues and future directions in research related to subsecond thermophysics. One of the main recommendations was to concentrate on continued development of new and more accurate dynamic measurement techniques.

Up to this time, we have used our submicrosecond pulse-heating system [2], which permitted us to achieve very high temperatures with heating rates of $10^9\,\mathrm{K \cdot s^{-1}}$, but the uncertainties of measured quantities were relatively high. Now we have developed a second, slower pulse-heating system to obtain more accurate measurements around the melting point of the sample and into the liquid phase. The heating rates applied in this system are 10^7 to $10^8\,\mathrm{K \cdot s^{-1}}$, which are similar to those used in the

[1] Institut für Experimentalphysik, Technische Universität Graz, Petersgasse 16, A-8010 Graz, Austria.

0195-928X/92/0700-0699$06.50/0

isobaric expansion experiment (IEX) in Los Alamos [3]. The apparatus in Graz uses water as the pressure medium, while the IEX uses compressed argon gas. Both experiments are capable of achieving pressures of up to 5000 bar.

The slow apparatus enables us to perform more accurate measurements of thermophysical properties extended to lower temperatures than with the faster system, and our new techniques permit us to obtain new information about the heated metal samples such as sound speed, emissivity, and vapor pressure.

2. EXPERIMENTAL

2.1. The Discharge Circuit and Current and Voltage Measurements

Wire and tube-shaped metal samples are resistively self-heated with a RCL discharge circuit, as shown in Fig. 1. Energy is stored in a capacitor bank, with capacitance variable from 240 to 500 μF. The bank may be charged up to 10 kV. Bank discharge and crowbar operations are controlled with ignitron switches. To obtain a low inductivity and to avoid ground loop problems, the main part of the discharge circuit is configured coaxially and grounded at a single point.

The shape of the rectangular current pulse is controlled by the bank circuit and independent of the changing resistance of the sample. A typical current pulse is shown in Fig. 2. After a controlled delay time the discharge is interrupted by crowbar operation.

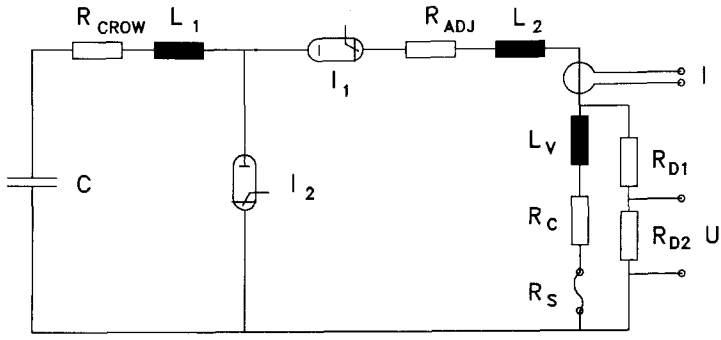

Fig. 1. Functional diagram of the capacitor discharge circuit including current and voltage measuring systems. C, capacitor; R_{CROW}, crowbar resistor; R_{ADJ}, adjustable resistor; $L_{1,2}$, inductance; I_1, discharge ignitron; I_2, crowbar ignitron; L_V, inductance of the vessel; R_C, resistance of the contacts; R_S, resistance of the sample; R_D, voltage divider.

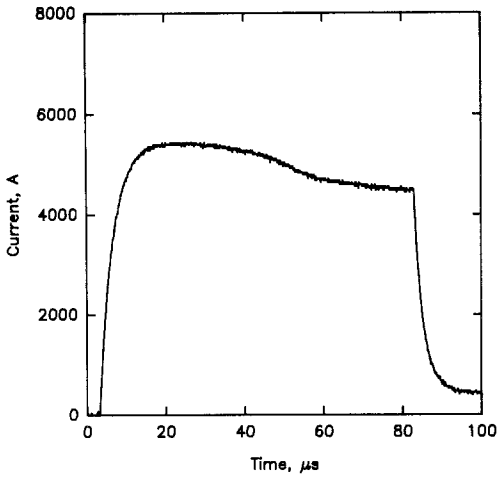

Fig. 2. A typical trace of a current waveform versus time. The pulse length is 80 μs, controlled by the crowbar operation.

As indicated in Fig. 1, the current through the sample is measured with a Pearson probe. This current transformer adds no load resistance to the circuit, and the output is electrically isolated from the discharge circuit. The uncertainty in the current measurements does not exceed ±1.5%.

The voltage measurement is made using a coaxial ohmic voltage divider (50 kΩ:50 Ω). The resistive and inductive voltage drop across the sample and the discharge vessel is measured. An example of a typical measured voltage trace is shown in Fig. 3. The measured voltage U is made up of a sum of resistive voltage drop across the sample R_S and contact resistance R_C, as well as inductive components caused by the changing of current I through sample L_S and cell L_V and the changing of inductance of the sample:

$$U(t) = I(t)\, R_S(t) + L_V \frac{dI(t)}{dt} + I(t)\, R_C + L_S \frac{dI(t)}{dt} + I(t) \frac{dL_S(t)}{dt} \qquad (1)$$

where t is time. The last two terms contribute less then ±1% to the measured voltage. The contact resistance is measured before the experiment, and a correction is made which is of the order of 1%.

The jump at the beginning of the signal in Fig. 3 comes from the second term on the right side of Eq. (1), but L_V is unknown. In order to compensate for it, we calculate at time $t = 0$

$$U(0) = I(0)\, R_S + L_V \frac{dI(t)}{dt} \qquad (2)$$

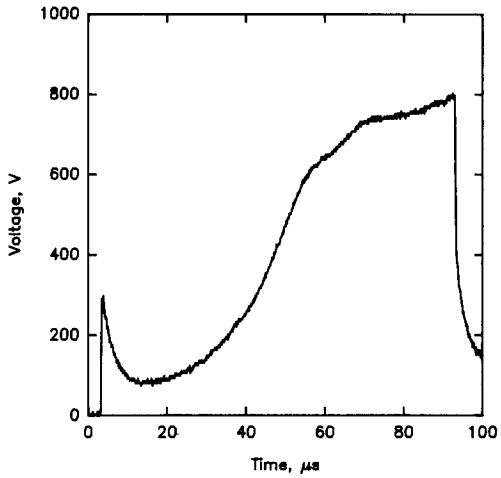

Fig. 3. A typical voltage waveform plotted versus time.

with $I(0)=0$ at the first instant. The change in current with time is known from the current measurements. The uncertainty of the voltage measurements does not exceed $\pm 2\%$.

Since we share the screen room with our fast system it is necessary to use coaxial measuring lines placed in copper tubes to prevent interference. The signals are lead to digital oscilloscopes for data aquisition, with all measuring lines having rise times of less than 100 ns.

From these electrical measurements we can calculate the time dependence of enthalpy and resistance of the sample. The uncertainty of the obtained values is estimated to be $\pm 3\%$ for specific enthalpy and $\pm 3\%$ for the specific electrical resistivity without volume correction.

2.2. Temperature and Expansion Measurement

We have constructed a new, very sensitive, and fast (response time, 100 ns) pyrometer to extend our measurement range to lower temperatures. This pyrometer resolves the melting plateau of copper, the highest fixed point of the International Temperature Scale of 1990 [4].

A lens produces a magnified image of the wire or tube at the rectangular entrance of an optical fiber. The light passes through the fiber and into an optical system with lenses and a narrow-band interference filter to select the wavelength. From the narrow-band filter the light enters a PIN photodiode detector. The resulting signal is amplified by a fast operational amplifier with linear and logarithmic output.

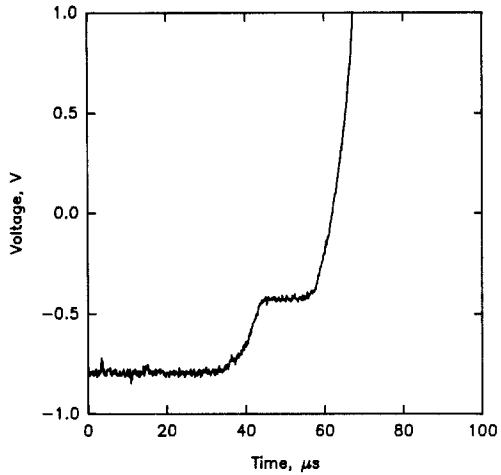

Fig. 4. Pyrometer output corresponding to surface radiance of the sample versus time for nickel, detected at a wavelength of 850 nm.

Our pyrometer is "self-calibrated" with the plateau of a melting transition. When calibrating with a melt plateau, it is important to have a high sensitivity, especially for metals with low melting points. Figure 4 shows the melting plateau of nickel measured at a wavelength of (850 ± 10) nm with a silicon detector, with the pyrometer becoming sensitive at 1500 K. Figure 5 shows a temperature trace measured in the near-infrared at 1.5 μm

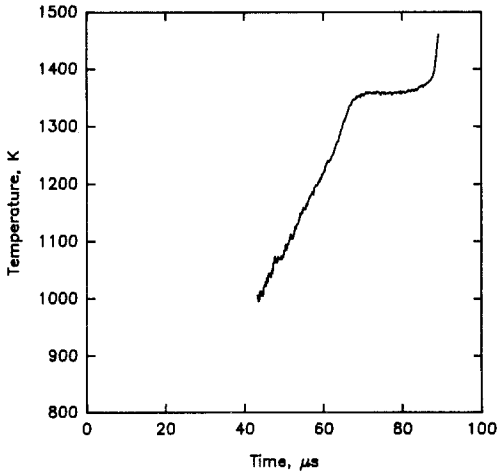

Fig. 5. Temperature versus time trace for a melting copper sample, measured at a wavelength of 1500 nm.

with a narrow-band filter of 20-nm bandwidth, using an indium–gallium–arsenide photodiode. Such a pyrometer is sensitive down to 1000 K. Many metals have their melting transition between 1000 and 2000 K, so we can now investigate many more materials with lower melting points than were possible previously. Temperature uncertainties are estimated to be up to $\pm 5\%$.

The thermal expansion is determined photographically. Photographs were taken with a high-speed camera using a kerr-cell shutter, with an exposure time of 30 ns. Many shots are required for these measurements, because only one photograph can be taken per shot. Increase in the diameter of the sample is related to the enthalpy at the instant the picture is taken. As the expansion takes place only radially, the measured diameters permit volumes and densities to be calculated.

Since our pressure vessel has only two windows, Melnitzky [5] has developed a method to obtain the temperature and the expansion measurement in one experiment. The experimental arrangement is shown in Fig. 6. The sample in the pressure vessel is backlighted by a flashlamp (2). The red and infrared parts of this light are blocked by an edge filter (5). A cold mirror (7) reflects the visible parts of the light emitted from the sample together with the background light from the flashlamp to the camera, which takes a photograph at a prechosen time. Only the red components of the sample self-radiation pass through the mirror (7) and enter the pyrometer. In this way the volume and the temperature can be detected simultaneously. This procedure increases the accuracy of our results.

The experimental uncertainty is estimated to be $\pm 3\%$ for volume measurements.

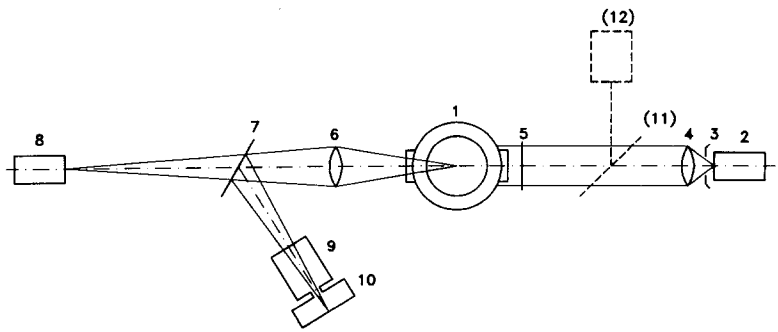

Fig. 6. Experimental setup for simultaneous measurement of expansion and temperature: 1, sample in the pressure vessel; 2, flashlight; 3, aperture; 4, lens; 5, edge filter; 6, lens; 7, cold mirror; 8, pyrometer; 9, kerr-cell shutter; 10, camera; 11, removable mirror; 12, lamp.

2.3. Spectral Emissivity Measurements on Liquid Metals

The temperature of the sample is obtained with the help of Planck's law. Since no spectral emissivity data for the liquid phase were available in the literature for nickel, we made additional measurements with metal tubes. Because of the high heating rate, the tube retains its shape into the liquid phase. This is demonstrated by short-time photographs taken of the pulse-heated tubes during heating. Light coming from inside the tube is measured at the same time the surface radiation is measured. At the melting plateau, the ratio of the time-resolved records of blackbody radiation from inside the tube I_{BB} and surface radiation I_{SF} are normalized by the spectral emissivity at the melting point $\varepsilon_{\lambda,M}$, taken from the literature (known only for a limited number of metals). This permits cancellation of the geometrical factors. The spectral emissivity ε_λ in the liquid state is determined by Eq. (3):

$$\varepsilon_\lambda = \varepsilon_{\lambda,M} \frac{I_{SF}}{I_{BB}} \tag{3}$$

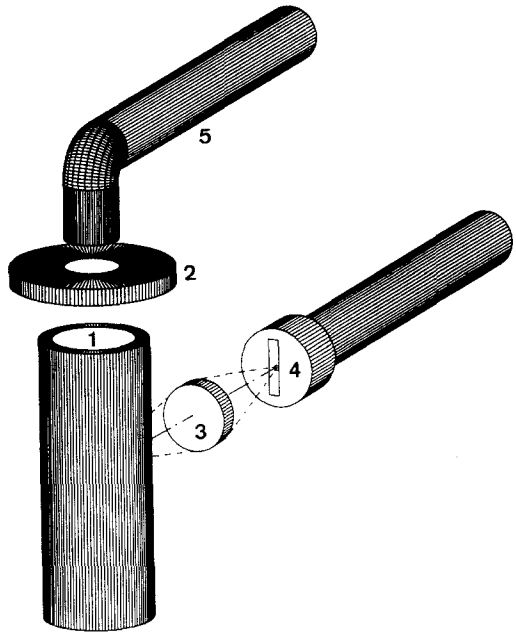

Fig. 7. Schematic representation of the spectral emissivity measurement for liquid metals: 1, tube-shaped sample; 2, aperture; 3, lens; 4, optical fiber (rectangular) to pyrometer 1; 5, light fiber (circular) to pyrometer 2.

The experimental arrangement used for the spectral emissivity measurements of liquid metals is shown in Fig. 7. The pyrometer 1 with the rectangular optical fiber detects the surface radiation of the sample. At the same time the pyrometer 2 with the circular optical fiber detects the black-body radiation of the sample. The circular lightfiber, looking down the axis of the tube, is mounted on the sample holder close to the end of the tube. The obtained emissivity values of the liquid phase are estimated to be accurate to $\pm 5\%$.

2.4. Measurement of the Speed of Sound

Figure 8 shows the experimental arrangement used for the speed of sound measurements. The sound wave in the sample is driven by a bullet fired from a rifle. This bullet first passes through the upper laser beam. Interrupting the laser beam causes the heating process to begin. As the sample is heated the bullet impacts the sample holder driving a sound wave into the sample. Simutaneously the bullet interrupts the second laser beam. During the time the bullet is traveling from the first to the second laser beam, the sample has been heated up to a certain temperature and the heating process has been stopped by bank crowbar.

When the bullet impacts the sample holder, the sample is at a uniform, homogeneous temperature. The uniformity of the sample is checked at the

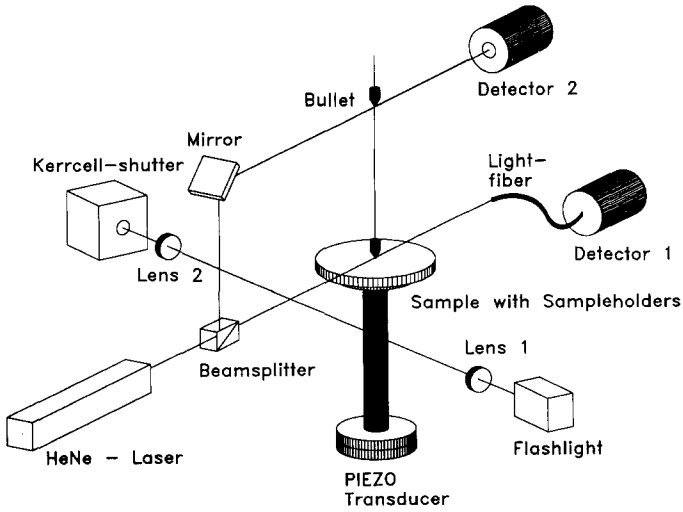

Fig. 8. Perspective drawing of the experimental setup used to measure sound speed.

impact time by taking a photograph of the sample. The sound wave now travels along the sample and is detected by a piezoelectric pressure transducer at the side opposite the source. The time required to pass through the sample holder and the response time of the pressure transducer are known from measurements with a cold sample and can be compensated for.

Figure 9 shows typical traces taken during a sound speed measurement. At point A (lower trace) heating is initiated. At point B the bullet impacts the sample holder and the sound wave is driven through the sample holder and into the sample. At point C the sound wave reaches the piezoelectric pressure transducer. From the time needed to pass through the sample the sound speed in the sample can be calculated with an accuracy of $\pm 10\%$.

2.5. Measurement of Vapor Pressure

Another new measurement is that of vapor pressure. Since the sample is contained in a high-pressure vessel with a maximum capability of 0.5 GPa, it is possible to investigate pressure dependencies. If the metal sample is heated to the boiling point at different ambient pressures, the binodial line of the phase diagram is passed and superheated states are reached. By crowbarring the heating current, and thus suppressing the vaporization, the energy input becomes zero and there is no energy left for

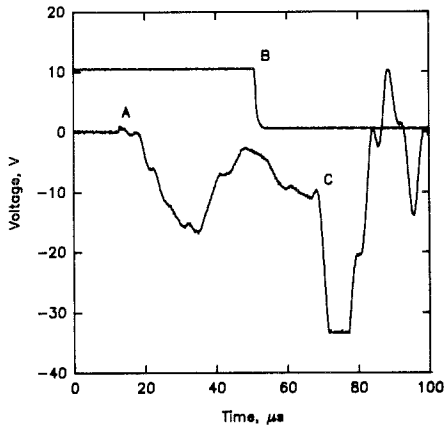

Fig. 9. Sound-speed measurement: typical traces of the voltages indicating the interrupt of the laser beam and the response of the pressure transducer plotted versus time.

the so-called phase explosion. The temperature decreases and remains constant for some time what should be the binodial temperature. We have fitted Hultgren and co-workers' [6] values for vapor pressure p as a function of temperature T up to 1 bar with the equation

$$\ln(p) = A - \frac{B}{T} \tag{4}$$

with A and B as coefficients. Our values lie very close to this line. First results on the vapor pressure of liquid cobalt will be reported elsewhere [7]. The pressure measurement has an uncertainty of $\pm 2\%$.

3. PRELIMINARY RESULTS

3.1. Spectral Emissivity of Liquid Nickel at 850 nm

Shown in Fig. 10 are our first results for measurements of spectral emissivity at 850 nm for nickel in the temperature range 1726 to 2250 K. The corresponding least-squares fit to this data is given by

$$\varepsilon_\lambda = 0.47448 - 8.0 \times 10^{-5}\, T \tag{5}$$

which shows ε_λ to be a slightly decreasing linear function of T.

The reference point $\varepsilon_{\lambda,\mathrm{M}}$ was measured by Righini [8]. Shown in Fig. 11 is the deviation of true temperature of liquid nickel from that found

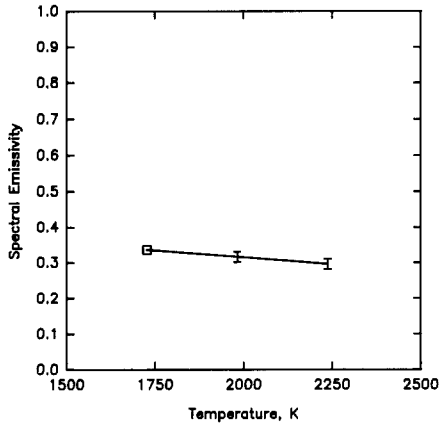

Fig. 10. Spectral emissivity versus temperature of liquid nickel at a wavelength of 850 nm.

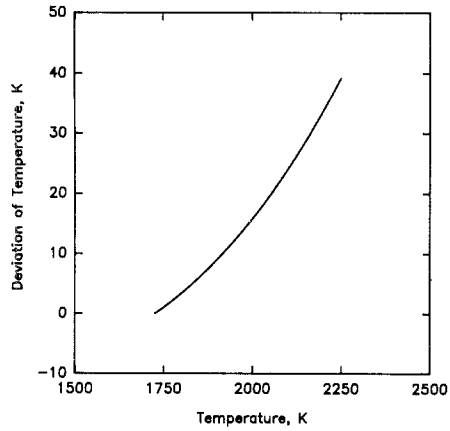

Fig. 11. Deviation of true temperature from that calculated with constant emissivity plotted versus true temperature for liquid nickel.

with the assumption of a constant spectral emissivity. At the true temperature of 2200 K, the assumption of constant emissivity leads to a temperature that is 35 K too high, corresponded to 1.6%. Further investigations on other metals and extension of the measurement range will be made in the future.

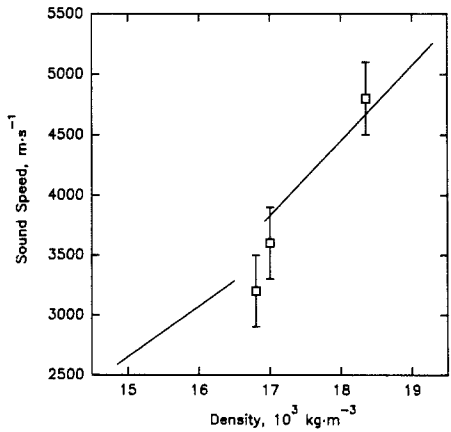

Fig. 12. Sound velocity versus density for tungsten. Values from this work are shown as open squares, the values of Hixson and Winkler [9] as a solid line.

3.2. Sound Speed in Tungsten

Figure 12 shows first results for measured sound velocities of solid tungsten plotted against density. Sound speed in tungsten up to the melting point of 3680 K have been obtained. Our data agrees with the measured values of Hixson and Winkler [9] within quoted error bars. To obtain data for the liquid phase some experimental details will have to be changed, because the sound wave dissipates strongly in the molten state. Further investigations will be performed with optical diagnostic techniques. A new high-speed framing camera with a video imaging system is now under construction.

4. CONCLUSION

A new microsecond pulse-heating system has been developed to investigate the properties of solid and liquid metal samples. We measure enthalpy, temperature, volume, and electrical resistivity. Additionally, we have now developed techniques to measure sound speed, spectral emissivity, and vapor pressure.

This work is continuing and shall be extended to obtain critical-point data and other thermophysical properties such as thermal conductivity of liquid metals.

REFERENCES

1. A. Cezairliyan, G. R. Gathers, A. M. Malvezzi, A. P. Miiller, F. Righini, and J. W. Shaner, *Int. J. Thermophys.* **11**:819 (1990).
2. R. Gallob, H. Jäger, and G. Pottlacher, *Int. J. Thermophys.* 7:139 (1986).
3. G. R. Gathers, J. W. Shaner, and R. K. Brier, *Rev. Sci. Instrum.* **47**:471 (1976).
4. H. Preston-Thomas, *Metrologia* **27**:3 (1990).
5. S. Melnitzky, Diploma thesis (Technische Universität Graz, Graz, 1991).
6. R. Hultgren, P. D. Desai, D. T. Hawkins, M. Gleiser, K. K. Kelley, and D. D. Wagman, *Selected Values of the Thermodynamic Properties of the Elements* (ASM, Metals Park, Ohio, 1973).
7. H. Hess, E. Kaschnitz, and G. Pottlacher, in press.
8. F. Righini, unpublished data (1980).
9. R. S. Hixson and M. A. Winkler, *Int. J. Thermophys.* **11**:709 (1990).